

Directional Pumping of Coherent Phonons and Quasiparticle Renormalization in a Dirac Nodal-Line Semimetal

Chenyu Wang,^{1,2} Daqiang Chen,^{1,2} Yaxian Wang^{1,*} and Sheng Meng^{1,2,3,†}

¹*Beijing National Laboratory for Condensed Matter Physics and
Institute of Physics, Chinese Academy of Sciences, Beijing 100190, China*

²*School of Physical Sciences, University of Chinese Academy of Sciences, Beijing 100190, China*

³*Songshan Lake Materials Laboratory, Dongguan, Guangdong 523808, China*

 (Received 20 November 2024; revised 6 March 2025; accepted 21 April 2025; published 14 May 2025)

Identifying efficient pathways to modulate quantum coherence is a crucial step toward realizing ultrafast switching of macroscopic orders, which requires the microscopical understanding of the interplay between multidegrees of freedom. Here, we demonstrate an all-optical method to control the coherent electron and lattice excitation in a prototypical nodal-line semimetal ZrSiS. We show the displacive excitation of two coherent Raman-active phonon modes, which results in a mode-selective renormalization of its topological band structure comparable with previous experimental observations. We subsequently realize an effective manipulation of the coherent lattice vibration, not only for their amplitude, but also a π -phase shift by tuning the laser intensity and frequency. We pinpoint that such a phase shift originates from the photoinduced carrier redistribution and can, in turn, determine the quasiparticle renormalization, for example, to induce an ultrafast topological Lifshitz transition, which we anticipate can be detected by pump-probe transport measurements. These results address the requirements for a directional pumping of coherent phonons with laser fields and provide the opportunity to explore exotic nonequilibrium physics.

DOI: 10.1103/PhysRevX.15.021053

Subject Areas: Computational Physics,
Condensed Matter Physics

Driving lattice vibration with a high degree of spatial and temporal coherence via strong light-matter interactions has evolved into a unique knob to control ultrafast phenomena and exotic physical phases [1–6]. In stark contrast to the thermal fluctuation in equilibrium, the vibrational coherence often produces a nonthermal change in macroscopic quantum states such as topology [7–11], magnetism [12,13], and superconductivity [14–16]. For example, ultrafast nonthermal engineering of the band topology has been experimentally realized via light-induced coherent phonon excitation in several typical topological semimetals such as WTe₂, MoTe₂, and ZrTe₅ [7,8,17–19], bringing us closer to the horizon of unprecedentedly fast and efficient information process technologies [2]. In this context, the phonons are primarily launched in terms of a “displacive” excitation, where the photoexcited carriers exert a non-equilibrium force onto the atoms, resulting in coherent oscillation around a new distorted structure (Fig. 1). Within

this picture, the responses of atomic and electronic degrees of freedom are closely intertwined and mutually dependent [3,20]. In particular, the lattice geometry can be pumped to distort either “positively” or “negatively” along the phonon coordinate, in which the atoms are relocated into different configurations as depicted in Fig. 1, consequently inducing disparate electronic properties such as oppositely polarized ferroelectricity and magnetization [21,22]. It is, thus, important to disentangle the coupled dynamics not only to decode the experimental observations, but also to identify effective pathways toward the ultrafast manipulation of the coherent response.

Meanwhile, in comparison with other characterization methods such as transport and angle-resolved photoemission spectroscopy (ARPES), the ultrafast dynamics upon optical excitation offers a great opportunity to resolve the strengths of electron-electron correlation and electron-lattice interaction [14,18,23], which is of great significance for topological electronic phases. For example, it has been observed in another family of quantum matter, i.e., topological nodal-line semimetals (NLSMs), that the Dirac quasiparticles are strongly renormalized by the changes in electronic screening after photoexcitation [24–26]. However, despite the previously proposed electron-electron interactions, it remains to be addressed how optical excitation modulates the lattice and how it interplays with the electrons under far-from-equilibrium conditions.

*Contact author: yaxianw@iphy.ac.cn

†Contact author: smeng@iphy.ac.cn

Published by the American Physical Society under the terms of the Creative Commons Attribution 4.0 International license. Further distribution of this work must maintain attribution to the author(s) and the published article's title, journal citation, and DOI.

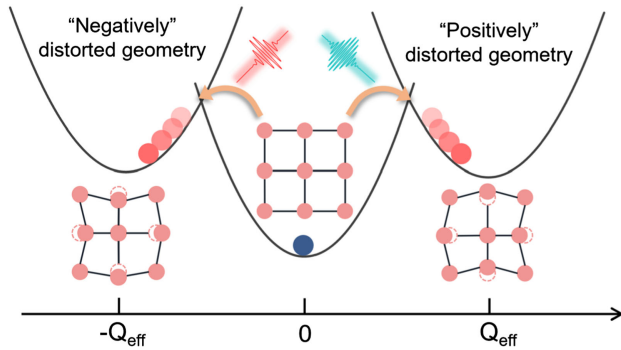


FIG. 1. Light-induced coherent control of the lattice geometry through the displacive excitation of coherent phonons (DECP). The photoexcitation induces a metastable lattice distortion along a specific phonon coordinate, as a result of the modification of the potential energy surface minimum from 0 to Q_{eff} . The direction of Q_{eff} determines the effective lattice geometry and the corresponding nonequilibrium electronic properties.

Although contributing to the understanding of the displacive excitation of coherent phonons (DECP), theoretical methods based on phenomenological models are severely limited in describing the nonequilibrium dynamics for the lack of information at a *truly* excited state [27,28]. In this regard, a microscopic study that includes the interactions with external field and treats the nonequilibrium electron and lattice dynamics on the same footing, for example, by real-time time-dependent density functional theory in combination with Ehrenfest molecular dynamics simulation (TDDFT-MD), is urgently needed.

In this work, we aim to predict coherent phonon excitation without *ad hoc* assumptions and disentangle the coupled lattice and electron dynamics upon photoexcitation in a prototypical nodal-line semimetal ZrSiS using TDDFT-MD simulation [29–34]. By monitoring the time evolution, we obtain a displacive excitation of two coherent Raman-active phonons. Such light-induced atomic motion provides a dynamic driving field for the electrons, leading to a nonthermal modulation in the topological band structure, the amplitude of which is comparable with previous time-resolved ARPES experiments. Moreover, the ultrafast band renormalization exhibits a sensitivity in the phase of the collective atomic motion. We subsequently elucidate in detail the effects of various parameters, including the laser intensity and frequency, to achieve nonequilibrium states with desired features. Remarkably, when we vary the pump frequency, we observe a π -phase shift in the coherent phonon oscillation and, meanwhile, a completely different behavior in the electronic state, undetected in previous studies. Based on these, we propose an ultrafast topological Lifshitz transition under certain pump conditions, which we anticipate can be detected by time-resolved multidimensional photoemission spectroscopy and transport measurements. Finally, we pinpoint the pivotal role of photoinduced

charge carrier redistribution and provide a general protocol for the DECP process to determine the coherent lattice responses.

I. MODE-SPECIFIC AND COHERENT LATTICE EXCITATION

Bulk ZrSiS crystallizes in a tetragonal structure with the $P4/nmm$ symmetry (space group No. 129) [35]. As a prototypical material in the family of nodal-line semimetals, its band structure features the Dirac loops formed by the crossing of the conduction band and valence band near Fermi level (E_F) [36,37], shown in Fig. 2(a). These linearly dispersed Dirac quasiparticles featuring a unique Fermi velocity are dominant in determining the ground state properties. Besides, we note the electron pocket at Γ that sits about 0.1 eV above E_F might also interact with the Dirac quasiparticles through delicate band engineering, suggesting possible topological Lifshitz transition and interfering in, for instance, the transport process [38].

We use a Gaussian enveloped laser pulse centered at 1.55 eV with an intensity 3.91 mJ/cm^2 [yellow curve in Fig. 2(b)], to pump the system out of equilibrium (see Supplemental Material Sec. S1 for a detailed description of our theoretical framework [39]). To resolve the coherent phonon excitation, we track the transient response of the ZrSiS lattice by projecting the real-time atomic motion onto its vibrational eigenmodes. As shown in Fig. 2(b), only two phonon modes are driven to large amplitudes and show nearly perfect coherent motion. These two modes oscillate, respectively, with a frequency of 5.67 and 8.59 THz, displaying a slight softening of approximately 2% compared with their ground state values. Such dressed coherent atomic motions can be attributed to a sudden change in the screening effect after photoexcitation and, subsequently, the feedback of the phonon excitation upon the electron states, which are expected to be closer to the experimental observations (see Supplemental Material Sec. S2 for details [39]). While microscopic models can be designed to capture similar effects [40], most of them rely on phenomenological parameters and are, thus, less predictive and inaccurate in some cases. By analyzing the phonon spectrum, we find these two modes are fully symmetric with their corresponding atomic motions shown in Fig. 2(e), in consistent with the polarized Raman measurement of the A_{1g}^1 and A_{1g}^2 phonons [41].

Given that the lattice vibration is in a highly coherent manner, we can describe its dynamics in the time domain with a normal mode cosine function: $Q_{q\nu}(t) = A_{q\nu} \cos(\omega_{q\nu}t + \phi_{q\nu}) + Q_{q\nu,\text{eff}}$, where $A_{q\nu}$, $\omega_{q\nu}$, and $\phi_{q\nu}$ refer, respectively, to the amplitude, frequency, and phase of the coherent phonon oscillation with wave vector \mathbf{q} and mode index ν . Here, we choose $A_{q\nu}$ to be positive and set the peak time of the laser pulse as $t = 0$. Besides, the lattice geometry also experiences a shift in its quasiequilibrium coordinate from 0 to $Q_{q\nu,\text{eff}}$ as in the DECP

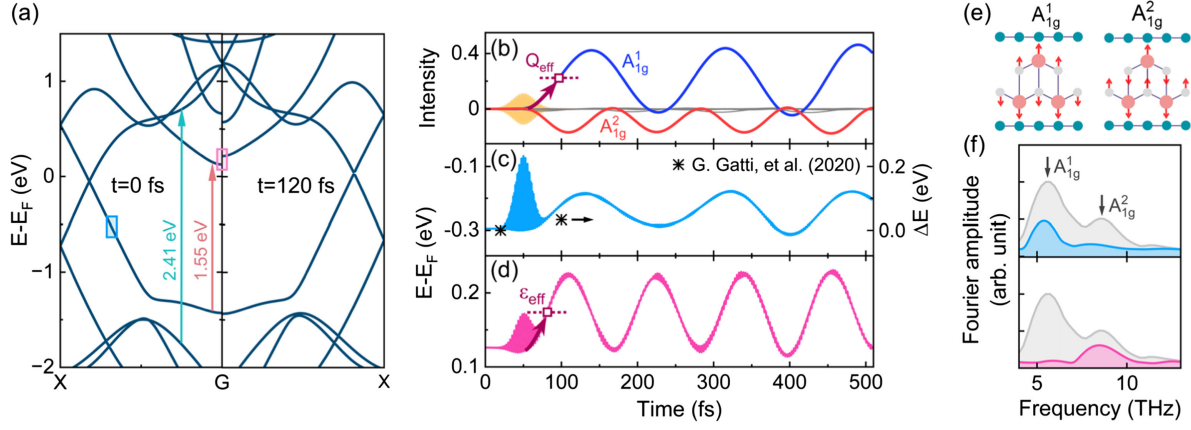


FIG. 2. (a) Transient band structure at 0 (i.e., the ground state) and 120 fs, with the states of our interest (SOIs) highlighted by squares. The two pump energies used in our simulations and the corresponding interband transitions are illustrated by the colored arrows. (b) Real-time atomic motion upon photoexcitation projected onto the eigenvectors of all phonon modes after pumping with a 1.55 eV laser pulse (yellow). While all other modes keep almost silent (gray curves), only two Raman-active A_{1g}^1 (blue) and A_{1g}^2 (red) modes are excited to oscillate coherently around a metastable distorted structure Q_{eff} denoted by the curved arrow. (c),(d) Time evolution of the SOIs showing a clear periodic oscillation with a time-averaged modulation ϵ_{eff} . The experimentally observed renormalization of the Dirac quasiparticles ΔE in a similar NLSM ZrSiSe is also shown for comparison [24]. (e) Vibrational eigenvectors of the two dominant phonon modes. (f) Fourier amplitude spectra of the oscillatory component of the electronic response shown in (c) (top) and (d) (bottom). The gray-shaded area corresponds to the Fourier spectrum of the periodic atomic motion with the arrows indicating the frequency of the A_{1g} phonons. The broadening of the peaks is a numerical outcome of the Fourier transformation instead of a physical indication of damping effects.

mechanism (Fig. 1). It should be noted that the oscillation phase is a unique and significant information available only in the nonequilibrium coherent regime, which is smeared out under thermal equilibrium when atoms oscillate in a phase-random manner [42]. Moreover, the phase shows a one-to-one correspondence with the direction of Q_{eff} , i.e., $\phi = 0$ ($\phi = \pi$) at negative (positive) Q_{eff} (Fig. 1). In particular, Q_{eff} is positive for A_{1g}^1 but negative for A_{1g}^2 mode, and, accordingly, their oscillation develops a π -phase shift.

II. COHERENT-PHONON-DRIVEN BAND RENORMALIZATION

Now we come to the ultrafast renormalization of the electronic structure, for which we show the transient band dispersion before ($t = 0$ fs) and after ($t = 120$ fs) the optical excitation, shown in Fig. 2(a). We label the near-Fermi-level electrons as states of our interest (SOIs) for simplicity, marked by the colored square in Fig. 2(a), with a special focus on the Fermi velocity of the Dirac quasiparticles and the energy level of the zone-center electron pocket. On top of the ultrafast response to the external field within the laser duration, we uncover an after-pulse periodic oscillation of the SOI energies. From performing a fast Fourier transform analysis, we reveal that the Dirac state vibrates at a frequency of 5.57 THz close to the frequency of the A_{1g}^1 mode, while the electron pocket at Γ oscillates concomitantly with the A_{1g}^2 mode with a frequency of 8.42 THz [Fig. 2(f)], indicating the lattice and

electrons are coupled in a highly selective manner. Notably, such coherent-phonon-induced renormalization of the Dirac quasiparticles has transiently reached approximately 80 meV on an ultrafast timescale after photoexcitation, which is comparable with previous experiment observations of about 30 meV in another similar NLSM ZrSiSe [24], shown in Fig. 2(c). Moreover, the Fermi velocity of the Dirac particles, a fundamental quantity essential for the material functional properties, is also substantially modified (see Supplemental Material Sec. S3 for the structure dependence of the Fermi velocity [39]). While the band renormalization in experiment was mainly ascribed to the change in the couplings among electrons, our results suggest a similar effect can be achieved in these NLSMs through coupling with the coherent lattice vibration.

On the other side, such band renormalization is stronger than that induced by thermal phonons, which we estimate to be around 10 meV (see Supplemental Material Sec. S4 for the estimation of electron self-energy [39]). In the nonequilibrium coherent-phonon regime, the dynamical modulation on the electronic state can be described as [43] $\epsilon_{i,k}(t) = \epsilon_{i,k}^0 + \sum_{qv} \sqrt{[(2\omega_{qv})/(\hbar)]} g_{i,k}^{qv} Q_{qv}(t)$, where $g_{i,k}^{qv}$ represents the mode-resolved electron-phonon coupling matrix element (see Sec. S3 for details [39]). Under equilibrium, the incoherent atomic motions are canceled out by each other, namely, $Q_{qv}(t) = 0$, and, consequently, lead to no net contribution to the band structure renormalization [44,45]. Therefore, such coherent and mode-specific phonon excitation offers a compelling nonthermal route to achieve unconventional optical modulation.

Aside from the periodic oscillations, we find the SOIs also accumulate a time-averaged effect arising from the displacive nature of the coherent phonons, which we characterize as

$$\epsilon_{\text{eff}}^{i,k} = \langle \epsilon_{i,k}(t) \rangle \sim \epsilon_{i,k}^0 + \sqrt{\frac{2\omega_{qv}}{\hbar}} g_{i,k}^{qv} Q_{qv,\text{eff}} \quad (1)$$

where $\langle \dots \rangle$ indicates the time average and we drop the summation since the coupling here is highly selective. The effective lattice distortion and, thus, the dressed state, for example, Dirac quasiparticles with well-tuned Fermi velocity, could have a lifetime of hundreds of femtoseconds depending on the relaxation rate of the excited electrons and induce measurable nonequilibrium effects (see Secs. S5 and S6 [39] for our detailed analysis on the effect of the decay processes).

III. OPTICAL MANIPULATION

We emphasize that, in the regime of electron-coherent-phonon coupling, the single-particle eigenvalue is proportional to Q_{eff} , i.e., highly sensitive to the phase of the collective atomic motion. This effect is absent in the conventional electron-phonon coupling pictured by the perturbation theory and, thus, provides a unique advantage in optical manipulation. While a “positive” direction of a phonon mode is arbitrarily defined in theory, it physically corresponds to the expansion or compression of specific bonds and the relocation of the charge distribution as in Fig. 1 [46], thus leading to a different behavior in the

electronic states (see Supplemental Material Sec. S3 [39]). Therefore, it is necessary to identify effective ways to manipulate the phase, amplitudes, and effective displacement of the displacively excited coherent phonons, in order to access nontrivial state inaccessible in equilibrium.

On the ground of this, we study the dependence of the coherent phonon dynamics on the pump laser wavelength, using 800 (1.55 eV) and 514 nm (2.41 eV) as showcases, with a wide range of pump fluences. We find the A_{1g}^1 mode always exhibits a π -phase oscillation, with an enhanced amplitude A and effective lattice distortion Q_{eff} upon strong field excitation at both frequencies of 1.55 and 2.41 eV (Supplemental Material Sec. S7 [39]). Notably, the behavior of the phonon amplitude and the effective distortion deviates from the linear trend especially upon strong field excitation. More importantly, the increased amplitude and Q_{eff} can lead to an enhanced renormalization of the Dirac quasiparticles, particularly their Fermi velocity, resulting in an effect much stronger than that induced by purely electron-electron interactions (for details, see Supplemental Material Secs. S3 and S8 [39]). However, while a similar fluence dependence is observed on the magnitude of A and Q_{eff} for A_{1g}^2 mode [Fig. 3(b)], it is rather fascinating that the phase undergoes a sudden shift from 0 to π and Q_{eff} flips its direction from negative to positive, when we increase the photon energy as shown in Figs. 3(a) and 3(b). Meanwhile, the zone-center electron pocket is renormalized into different effective values ϵ_{eff} as shown in Fig. 4(a). This suggests that, accompanying the phase shift, the lattice is rectified into different

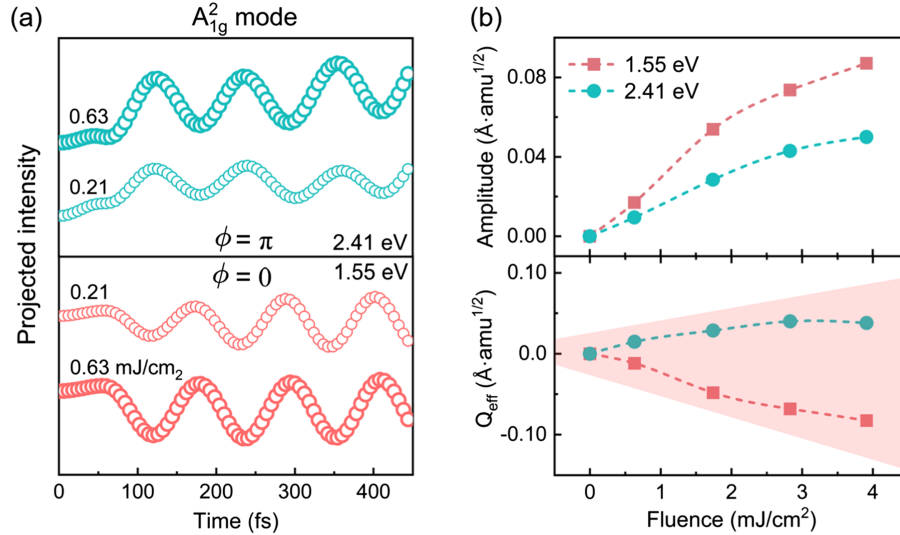


FIG. 3. Ultrafast control of the phonon phase, amplitude, and the effective lattice distortion in DECP. (a) Coherent phonon dynamics of the A_{1g}^2 phonon under various pump conditions. The phase undergoes a sudden phase shift and, meanwhile, the quasiequilibrium lattice coordinate is displaced to the opposite direction, when we increase the photon energy from 1.55 (bottom) to 2.41 eV (top). On the other side, the amplitude grows with enhanced pump intensity at all frequencies. (b) A detailed dependence of the oscillation amplitude A (top) and the metastable lattice distortion Q_{eff} (bottom) on the laser parameters. The color shading is a guide to the eye to show the trend, highlighting the double-sided displacive excitation of the A_{1g}^2 mode.

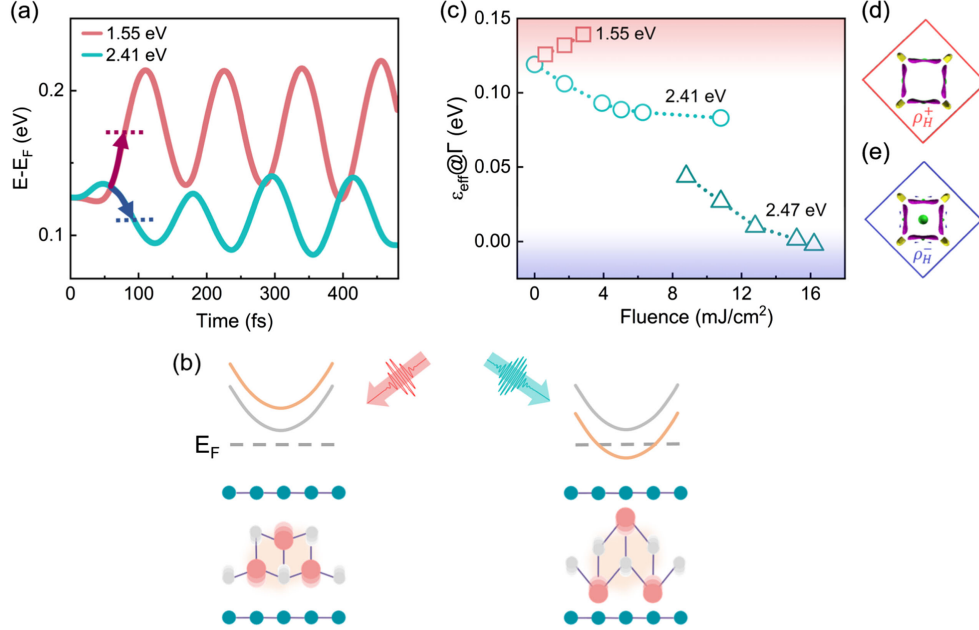


FIG. 4. Quasiparticle renormalization. (a) The oscillation of the zone-center electron pocket, which also develops a π -phase shift with increased pumping frequency and, meanwhile, the band renormalization accumulates an opposite time-averaged effect ϵ_{eff} as indicated by the colored arrows. (b) The distinct electronic structure dictated by the lattice dynamics. When the A_{1g}^2 mode oscillates with a 0 phase (π phase) under a 1.55 eV (2.41 eV) pumping, the distance between the adjacent Zr layers experiences a net compression (elongation), driving the electron pocket farther from (closer to) the Fermi surface. (c) Light-induced ultrafast engineering on Fermi surface topology. The zone center electron pocket would decrease its energy when pumped at frequencies near 2.41 eV. The ultrafast light-induced Lifshitz transition could be observed upon a suitable pump condition, for example, at 2.47 eV and 16.2 mJ/cm². The color shading corresponds to a change in the Fermi surface topology and the Hall conductivity ρ_H (d) before and (e) after the quantum Lifshitz transition.

configurations and, thus, induces distinctive electronic behavior as shown in Fig. 4(b). Intriguingly, when the net lattice distortion along A_{1g}^2 mode involves an elongation of the adjacent Zr layers as in the π -phase case at 2.41 eV pumping, the zone-center electron pocket is driven closer to E_F , with a possibility to penetrate the Fermi surface and triggering topological Lifshitz transitions [Fig. S2(c) in Supplemental Material Sec. S3 [39]]. Although the coherent phonon excitation has been observed in the pump-probe experiment [14,18], such phase-sensitive electronic behavior has rarely been reported in the context of DECP before.

For a detailed analysis, we calculate the ultrafast Fermi surface engineering with light. In Fig. 4(c), we show that the effective band renormalization gradually saturates with respect to the pump fluence and the zone-center electron pocket remains above the Fermi level at 2.41 eV excitation (see Supplemental Material Sec. S9 for details [39]). However, we find that slight tuning of the photon energy near 2.41 eV enables further control over the electron and lattice dynamics without disrupting the π -phase excitation of the A_{1g}^2 mode. Particularly, the band renormalization can be significantly enhanced at 2.47 eV excitation, where an abrupt change in the Fermi surface topology is predicted to occur above certain pump fluence (for more details, see Supplemental Material Sec. S10 [39]). In practice, such a

dynamical Lifshitz transition can be probed directly by time-resolved multidimensional photoemission spectroscopy and has been demonstrated in T_d -MoTe₂ [38]. Meanwhile, a light-induced phonon excitation accompanying a circular photogalvanic effect arising from the symmetry breaking in ZrTe₅ is observed [47]. However, in our case, the excitation of A_{1g} phonons inherits the lattice symmetry. As transport signatures, for example, the magnetoresistance and Hall conductivity, are a general metric to probe the charge polarity in a conductor [48,49], we simulate the in-plane Hall resistivity ρ_H with respect to lattice distortion, which is found to exhibit a sign flip from positive to negative, manifesting the reconstruction of the Fermi surface and the switch of the dominant carrier types (see Supplemental Material Sec. S11 for detailed analysis [39]). Although characterizing the transport signal with a picosecond resolution is challenging, the light-induced anomalous Hall effect in graphene [50] makes it an intriguing direction to bridge the nonequilibrium band topology with transient macroscopic properties.

IV. DISCUSSION

As introduced in the beginning, the direction of the DECP is phenomenologically dictated by the electron-phonon coupling strength of the excited electron-hole pairs;

we now seek to pin down the physical origin for the phase shift and the sign switch of the time-averaged displacement Q_{eff} . The photoexcited potential energy surface (PES) along the A_{1g}^2 phonon coordinate can be, in theory, described by the lattice potential containing electron-phonon coupling:

$$V(Q_{qv}) = \frac{1}{2}\omega_{qv}^2 Q_{qv}^2 + \sum_{i,k} \sqrt{\frac{2\omega_{qv}}{\hbar}} g_{i,k}^{q,\nu} \Delta f_{i,k} Q_{qv}, \quad (2)$$

where $\Delta f_{i,k}$ denotes the distribution function change before and after excitation. A straightforward definition of phonon displacement as $Q_{\text{eff}} \sim -\sum_{i,k} g_{i,k}^{q,\nu} \Delta f_{i,k}$ from Eq. (2) reveals that the total electron-phonon coupling strength carried by all the photoexcited electron-hole pairs determines the direction and magnitude of the PES shift. To verify our phenomenological model, we first calculate the excited energy landscape of A_{1g}^2 mode by artificially redistributing one electron from its valence band to the conduction band. In this case, the expression of Q_{eff} can be further simplified into $Q_{\text{eff}} \sim g_{v,k} - g_{c,k}$, where v and c refer to the valence and conduction band, respectively. As shown in Figs. 5(a) and 5(b), we indeed observe Q_{eff} with opposite directions depending on the electron-phonon coupling strength of the selected electron-hole pairs, namely, negative at $g_{v,k} - g_{c,k} < 0$ and contrarily positive at $g_{v,k} - g_{c,k} > 0$. Furthermore, we find in our TDDFT simulations the carriers are redistributed into different energy levels for laser frequency at $\hbar\omega = 1.55$ and 2.41 eV, where the dominant interband transitions are schematically denoted by the colored arrows in Fig. 2(a). We then extract the transient occupation number and sum up the electron-phonon coupling strength from all the photoexcited electron-hole pairs, from which we obtain the net lattice displacement with opposite signs, to be $Q_{\text{eff}} = -0.0483$ and $0.0287 \text{ \AA}\sqrt{\text{amu}}$, respectively, in well

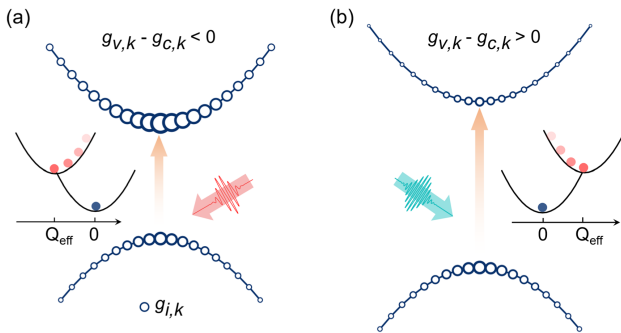


FIG. 5. Microscopic nonequilibrium control of DECP. The direction of the lattice distortion is determined by the mode-resolved electron-phonon coupling strength $g_{i,k}$ (navy open circles) and carrier redistribution. In the special case of relocating only one electron from valence to conduction band, Q_{eff} is determined to be negative at (a) $g_{v,k} - g_{c,k} < 0$ and contrarily positive at (b) $g_{v,k} - g_{c,k} > 0$. The carrier population can be effectively modulated by the photon frequency.

consistency with our TDDFT simulations. Taken together, the opposite displacive excitation of coherent phonons and, correspondingly, the phase shift are ascribed to different interband electron transitions that are tunable with light, which could be properly identified only at the inclusion of realistic excitation channels based on a precise description of the interaction with external laser field. Based on the above analysis, we attribute the sublinear fluence dependence observed in both the electron and phonon dynamics at 2.41 eV excitation primarily to the saturated electronic excitation at high laser intensity. Furthermore, in the case of 2.47 eV excitation, the saturation effect occurs at a much higher fluence, due to the fact that enhanced local density of state enables additional excitation channels, and, thus, both the coherent phonon oscillation and the band renormalization can be strengthened (see Secs. S9 and S10 for more details [39]).

More importantly, we have also demonstrated the ability to realize similar phase control in a completely different kind of compound of semiconducting WSe_2 , which not only further validates our microscopic description of DECP, but also provides an effective way toward the ultrafast engineering of nonequilibrium states across diverse quantum materials (see Sec. S13 for details [39]).

In conclusion, we take the nodal-line semimetal ZrSiS as a paradigmatic system to show the mutual dependence of the coherent atomic and electronic dynamics after photoexcitation. The displacive excitation of Raman-active A_{1g} phonons simultaneously modulates the topological band structure at the same frequency, as a direct manifestation of mode-resolved electron-phonon coupling beyond equilibrium. Intriguingly, we reveal an unreported dependence of the ultrafast electronic response on the phase of the collective atomic motion, where the time-averaged single-particle energy can be either lifted or reduced reliant on the oscillation phase, leading to distinctive macroscopic properties. We subsequently realize the effective manipulation of the coherent lattice dynamics with switchable phases by tuning the laser frequency and propose a non-trivial topological Lifshitz transition under certain pump conditions, which we anticipate can be detected by time-resolved transport measurements. Finally, we provide an explicit description on the microscopic origin of the directional pumping of coherent phonons, which can be generalized into other quantum materials. Our work offers a microscopic understanding of the ultrafast and mode-selective band renormalization via light-driven coherent phonons and provides insights into the optical control of structure-sensitive materials properties such as ferroelectricity, topology, charge density waves, and metal-insulator transitions.

ACKNOWLEDGMENTS

We acknowledge funding support from National Natural Science Foundation of China (No. 12025407,

No. 12474246, No. 12450401, and No. 92250303), Chinese Academy of Sciences (No. YSBR-047 and No. XDB33030100), and Ministry of Science and Technology (No. 2021YFA1400201).

-
- [1] A. Marciniak, S. Marcantoni, F. Giusti, F. Glerean, G. Sparapassi, T. Nova, A. Cartella, S. Latini, F. Valiera, A. Rubio, J. van den Brink, F. Benatti, and D. Fausti, *Vibrational coherent control of localized d-d electronic excitation*, *Nat. Phys.* **17**, 368 (2021).
- [2] C. Bao, P. Tang, D. Sun, and S. Zhou, *Light-induced emergent phenomena in 2D materials and topological materials*, *Nat. Rev. Phys.* **4**, 33 (2022).
- [3] M.-X. Guan, X.-B. Liu, D.-Q. Chen, X.-Y. Li, Y.-P. Qi, Q. Yang, P.-W. You, and S. Meng, *Optical control of multistage phase transition via phonon coupling in MoTe₂*, *Phys. Rev. Lett.* **128**, 015702 (2022).
- [4] X. T. Nguyen, K. Winte, D. Timmer, Y. Rakita, D. R. Ceratti, S. Aharon, M. S. Ramzan, C. Cocchi, M. Lorke, F. Jahnke, D. Cahen, C. Lienau, and A. De Sio, *Phonon-driven intra-exciton Rabi oscillations in CsPbBr₃ halide perovskites*, *Nat. Commun.* **14**, 1047 (2023).
- [5] T. Heinrich, H.-T. Chang, S. Zayko, K. Rosnagel, M. Sivis, and C. Ropers, *Electronic and structural fingerprints of charge-density-wave excitations in extreme ultraviolet transient absorption spectroscopy*, *Phys. Rev. X* **13**, 021033 (2023).
- [6] M. Basini, M. Pancaldi, B. Wehinger, M. Udina, V. Unikandanunni, T. Tadano, M. C. Hoffmann, A. V. Balatsky, and S. Bonetti, *Terahertz electric-field-driven dynamical multiferroicity in SrTiO₃*, *Nature (London)* **628**, 534 (2024).
- [7] E. J. Sie, C. M. Nyby, C. D. Pemmaraju, S. J. Park, X. Shen, J. Yang, M. C. Hoffmann, B. K. Ofori-Okai, R. Li, A. H. Reid, S. Weathersby, E. Mannebach, N. Finney, D. Rhodes, D. Chenet, A. Antony, L. Balicas, J. Hone, T. P. Devereaux, T. F. Heinz, X. Wang, and A. M. Lindenberg, *An ultrafast symmetry switch in a Weyl semimetal*, *Nature (London)* **565**, 61 (2019).
- [8] T. Konstantinova, L. Wu, W.-G. Yin, J. Tao, G. D. Gu, X. J. Wang, J. Yang, I. A. Zaliznyak, and Y. Zhu, *Photo-induced Dirac semimetal in ZrTe₅*, *npj Quantum Mater.* **5**, 80 (2020).
- [9] N. Aryal, X. Jin, Q. Li, A. M. Tsvetlik, and W. Yin, *Topological phase transition and phonon-space Dirac topology surfaces in ZrTe₅*, *Phys. Rev. Lett.* **126**, 016401 (2021).
- [10] L.-L. Wang, *Expansive open Fermi arcs and connectivity changes induced by infrared phonons in ZrTe₅*, *Phys. Rev. B* **103**, 075105 (2021).
- [11] D. Shin, A. Rubio, and P. Tang, *Light-induced ideal Weyl semimetal in HgTe via nonlinear phononics*, *Phys. Rev. Lett.* **132**, 016603 (2024).
- [12] A. S. Disa, J. Curtis, M. Fechner, A. Liu, A. von Hoegen, M. Först, T. F. Nova, P. Narang, A. Maljuk, A. V. Boris, B. Keimer, and A. Cavalleri, *Photo-induced high-temperature ferromagnetism in YTiO₃*, *Nature (London)* **617**, 73 (2023).
- [13] N. Wu, S. Zhang, D. Chen, Y. Wang, and S. Meng, *Three-stage ultrafast demagnetization dynamics in a monolayer ferromagnet*, *Nat. Commun.* **15**, 2804 (2024).
- [14] S.-L. Yang, J. A. Sobota, Y. He, D. Leuenberger, H. Soifer, H. Eisaki, P. S. Kirchmann, and Z.-X. Shen, *Mode-selective coupling of coherent phonons to the Bi2212 electronic band structure*, *Phys. Rev. Lett.* **122**, 176403 (2019).
- [15] E. Rowe, B. Yuan, M. Buzzi, G. Jotzu, Y. Zhu, M. Fechner, M. Först, B. Liu, D. Pontiroli, M. Riccò, and A. Cavalleri, *Resonant enhancement of photo-induced superconductivity in K₃C₆₀*, *Nat. Phys.* **19**, 1821 (2023).
- [16] C. J. Eckhardt, S. Chattopadhyay, D. M. Kennes, E. A. Demler, M. A. Sentef, and M. H. Michael, *Theory of resonantly enhanced photo-induced superconductivity*, *Nat. Commun.* **15**, 2300 (2024).
- [17] M. Y. Zhang, Z. X. Wang, Y. N. Li, L. Y. Shi, D. Wu, T. Lin, S. J. Zhang, Y. Q. Liu, Q. M. Liu, J. Wang, T. Dong, and N. L. Wang, *Light-induced subpicosecond lattice symmetry switch in MoTe₂*, *Phys. Rev. X* **9**, 021036 (2019).
- [18] P. Hein, S. Jauernik, H. Erk, L. Yang, Y. Qi, Y. Sun, C. Felser, and M. Bauer, *Mode-resolved reciprocal space mapping of electron-phonon interaction in the Weyl semimetal candidate Td-WTe₂*, *Nat. Commun.* **11**, 2613 (2020).
- [19] C. Vaswani, L.-L. Wang, D. H. Mudiyansele, Q. Li, P. M. Lozano, G. D. Gu, D. Cheng, B. Song, L. Luo, R. H. J. Kim, C. Huang, Z. Liu, M. Mootz, I. E. Perakis, Y. Yao, K. M. Ho, and J. Wang, *Light-driven Raman coherence as a nonthermal route to ultrafast topology switching in a Dirac semimetal*, *Phys. Rev. X* **10**, 021013 (2020).
- [20] E. M. Bothschafter, A. Paarmann, E. S. Zijlstra, N. Karpowicz, M. E. Garcia, R. Kienberger, and R. Ernstorfer, *Ultrafast evolution of the excited-state potential energy surface of TiO₂ single crystals induced by carrier cooling*, *Phys. Rev. Lett.* **110**, 067402 (2013).
- [21] M.-M. Yang and M. Alexe, *Light-induced reversible control of ferroelectric polarization in BiFeO₃*, *Adv. Mater.* **30**, 1704908 (2018).
- [22] A. S. Disa, M. Fechner, T. F. Nova, B. Liu, M. Först, D. Prabhakaran, P. G. Radaelli, and A. Cavalleri, *Polarizing an antiferromagnet by optical engineering of the crystal field*, *Nat. Phys.* **16**, 937 (2020).
- [23] Y. Huang, J. D. Querales-Flores, S. W. Teitelbaum, J. Cao, T. Henighan, H. Liu, M. Jiang, G. De la Peña, V. Krapivin, J. Haber, T. Sato, M. Chollet, D. Zhu, T. Katayama, R. Power, M. Allen, C. R. Rotundu, T. P. Bailey, C. Uher, M. Trigo, P. S. Kirchmann, E. D. Murray, Z.-X. Shen, I. Savić, S. Fahy, J. A. Sobota, and D. A. Reis, *Ultrafast measurements of mode-specific deformation potentials of Bi₂Te₃ and Bi₂Se₃*, *Phys. Rev. X* **13**, 041050 (2023).
- [24] G. Gatti, A. Crepaldi, M. Puppini, N. Tancogne-Dejean, L. Xian, U. De Giovannini, S. Roth, S. Polishchuk, P. Bugnon, A. Magrez, H. Berger, F. Frassetto, L. Poletto, L. Moreschini, S. Moser, A. Bostwick, E. Rotenberg, A. Rubio, M. Chergui, and M. Grioni, *Light-induced renormalization of the Dirac quasiparticles in the nodal-line semimetal ZrSiSe*, *Phys. Rev. Lett.* **125**, 076401 (2020).
- [25] N. Nilforoushan, M. Casula, M. Caputo, E. Papalazarou, J. Caillaux, Z. Chen, L. Perfetti, A. Amaricci, D. Santos-Cottin, Y. Klein, A. Gauzzi, and M. Marsi, *Photo-induced renormalization and electronic screening of*

- quasi-two-dimensional Dirac states in BaNiS₂*, *Phys. Rev. Res.* **2**, 043397 (2020).
- [26] S. Biswas, I. Petrides, R. J. Kirby, C. Oberg, S. Klemenz, C. Weinberg, A. Ferrenti, P. Narang, L. M. Schoop, and G. D. Scholes, *Photoinduced band renormalization effects in the topological nodal-line semimetal ZrSiS*, *Phys. Rev. B* **106**, 134303 (2022).
- [27] G. A. Garrett, T. F. Albrecht, J. F. Whitaker, and R. Merlin, *Coherent THz phonons driven by light pulses and the Sb problem: What is the mechanism?*, *Phys. Rev. Lett.* **77**, 3661 (1996).
- [28] X. Tong and M. Bernardi, *Toward precise simulations of the coupled ultrafast dynamics of electrons and atomic vibrations in materials*, *Phys. Rev. Res.* **3**, 023072 (2021).
- [29] E. Runge and E. K. U. Gross, *Density-functional theory for time-dependent systems*, *Phys. Rev. Lett.* **52**, 997 (1984).
- [30] S. Meng and E. Kaxiras, *Real-time, local basis-set implementation of time-dependent density functional theory for excited state dynamics simulations*, *J. Chem. Phys.* **129**, 054110 (2008).
- [31] C. Lian, M. Guan, S. Hu, J. Zhang, and S. Meng, *Photoexcitation in solids: First-principles quantum simulations by real-time TDDFT*, *Adv. Theory. Simul.* **1**, 1800055 (2018).
- [32] C. Lian, S.-J. Zhang, S.-Q. Hu, M.-X. Guan, and S. Meng, *Ultrafast charge ordering by self-amplified exciton-phonon dynamics in TiSe₂*, *Nat. Commun.* **11**, 43 (2020).
- [33] M. Guan, D. Chen, S. Hu, H. Zhao, P. You, and S. Meng, *Theoretical insights into ultrafast dynamics in quantum materials*, *Ultrafast Sci.* **2022**, 9767251 (2022).
- [34] R. Zhao, P. You, and S. Meng, *Ring polymer molecular dynamics with electronic transitions*, *Phys. Rev. Lett.* **130**, 166401 (2023).
- [35] L. M. Schoop, M. N. Ali, C. Straßer, A. Topp, A. Varykhalov, D. Marchenko, V. Duppel, S. S. P. Parkin, B. V. Lotsch, and C. R. Ast, *Dirac cone protected by non-symmorphic symmetry and three-dimensional Dirac line node in ZrSiS*, *Nat. Commun.* **7**, 11696 (2016).
- [36] J. Hu, Z. Tang, J. Liu, X. Liu, Y. Zhu, D. Graf, K. Myhro, S. Tran, C. N. Lau, J. Wei, and Z. Mao, *Evidence of topological nodal-line fermions in ZrSiSe and ZrSiTe*, *Phys. Rev. Lett.* **117**, 016602 (2016).
- [37] C. C. Gu, J. Hu, X. L. Chen, Z. P. Guo, B. T. Fu, Y. H. Zhou, C. An, Y. Zhou, R. R. Zhang, C. Y. Xi, Q. Y. Gu, C. Park, H. Y. Shu, W. G. Yang, L. Pi, Y. H. Zhang, Y. G. Yao, Z. R. Yang, J. H. Zhou, J. Sun, Z. Q. Mao, and M. L. Tian, *Experimental evidence of crystal symmetry protection for the topological nodal line semimetal state in ZrSiS*, *Phys. Rev. B* **100**, 205124 (2019).
- [38] S. Beaulieu, S. Dong, N. Tancogne-Dejean, M. Dendzik, T. Pincelli, J. Maklar, R. P. Xian, M. A. Sentef, M. Wolf, A. Rubio, L. Rettig, and R. Ernstorfer, *Ultrafast dynamical Lifshitz transition*, *Sci. Adv.* **7**, eabd9275 (2021).
- [39] See Supplemental Material at <http://link.aps.org/supplemental/10.1103/PhysRevX.15.021053> for supporting discussion on the decay process, additional calculations on the optical manipulation, and application of our theory to other materials.
- [40] M. Lakehal and I. Paul, *Microscopic description of displacive coherent phonons*, *Phys. Rev. B* **99**, 035131 (2019).
- [41] W. Zhou, H. Gao, J. Zhang, R. Fang, H. Song, T. Hu, A. Stroppa, L. Li, X. Wang, S. Ruan, and W. Ren, *Lattice dynamics of Dirac node-line semimetal ZrSiS*, *Phys. Rev. B* **96**, 064103 (2017).
- [42] M. Hase and M. Kitajima, *Interaction of coherent phonons with defects and elementary excitations*, *J. Phys. Condens. Matter* **22**, 073201 (2010).
- [43] F. Caruso and M. Zacharias, *Quantum theory of light-driven coherent lattice dynamics*, *Phys. Rev. B* **107**, 054102 (2023).
- [44] X. Hu and F. Nori, *Squeezed phonon states: Modulating quantum fluctuations of atomic displacements*, *Phys. Rev. Lett.* **76**, 2294 (1996).
- [45] C. Emeis, S. Jauernik, S. Dahiya, Y. Pan, C. E. Jensen, P. Hein, M. Bauer, and F. Caruso, *Phys. Rev. X* **15**, 021039 (2025).
- [46] S. Priyadarshi, I. Gonzalez-Vallejo, C. Hauf, K. Reimann, M. Woerner, and T. Elsaesser, *Phonon-induced relocation of valence charge in boron nitride observed by ultrafast x-ray diffraction*, *Phys. Rev. Lett.* **128**, 136402 (2022).
- [47] L. Luo, D. Cheng, B. Song, L.-L. Wang, C. Vaswani, P. M. Lozano, G. Gu, C. Huang, R. H. J. Kim, Z. Liu, J.-M. Park, Y. Yao, K. Ho, I. E. Perakis, Q. Li, and J. Wang, *A light-induced phononic symmetry switch and giant dissipationless topological photocurrent in ZrTe₅*, *Nat. Mater.* **20**, 329 (2021).
- [48] M. N. Ali, L. M. Schoop, C. Garg, J. M. Lippmann, E. Lara, B. Lotsch, and S. S. P. Parkin, *Butterfly magnetoresistance, quasi-2D Dirac Fermi surface and topological phase transition in ZrSiS*, *Sci. Adv.* **2**, e1601742 (2016).
- [49] S. N. Zhang, Q. S. Wu, Y. Liu, and O. V. Yazyev, *Magnetoresistance from Fermi surface topology*, *Phys. Rev. B* **99**, 035142 (2019).
- [50] J. W. McIver, B. Schulte, F.-U. Stein, T. Matsuyama, G. Jotzu, G. Meier, and A. Cavalleri, *Light-induced anomalous Hall effect in graphene*, *Nat. Phys.* **16**, 38 (2019).